Semiclassical spatial correlations in chaotic wave functions

Fabricio Toscano and Caio H. Lewenkopf

Instituto de Física, Universidade do Estado do Rio de Janeiro, R. São Francisco Xavier 524, 20559-900 Rio de Janeiro, Brazil
(Received 16 August 2001; published 8 February 2002)

We study the spatial autocorrelation of energy eigenfunctions $\psi_n(\mathbf{q})$ corresponding to classically chaotic systems in the semiclassical regime. Our analysis is based on the Weyl-Wigner formalism for the spectral average $C_\varepsilon(\mathbf{q}^+,\mathbf{q}^-,E)$ of $\psi_n(\mathbf{q}^+)\psi_n^*(\mathbf{q}^-)$, defined as the average over eigenstates within an energy window ε centered at E. In this framework C_ε is the Fourier transform in the momentum space of the spectral Wigner function $W(\mathbf{x},E;\varepsilon)$. Our study reveals the chord structure that C_ε inherits from the spectral Wigner function showing the interplay between the size of the spectral average window, and the spatial separation scale. We discuss under which conditions is it possible to define a local system independent regime for C_ε. In doing so, we derive an expression that bridges the existing formulas in the literature and find expressions for $C_\varepsilon(\mathbf{q}^+,\mathbf{q}^-,E)$ valid for any separation size $|\mathbf{q}^+-\mathbf{q}^-|$.

I. INTRODUCTION AND MOTIVATION

One of the key issues in the quantum chaos research is the quest for quantum fingerprints of the underlying classical dynamics of generic chaotic systems. In the last decade most studies of such kind were dedicated to spectral properties [1]. It is now established that, in general, systems with a classical chaotic dynamics are characterized by universal spectral fluctuations, which is the so-called Bohigas conjecture [2]. Much insight about this phenomenon was provided by the semiclassical approximation [3]. Specifically, it was shown that in the semiclassical regime [4–6] the energy level density autocorrelation function of a chaotic system, evaluated at energy separations encompassing several mean level spacings, displays similar statistical properties as those arising from ensembles of random matrices [7]. Starting from the random matrix side, advances in proving the connection to the spectral fluctuations of chaotic systems were also achieved [8,9]. Although a full proof of Bohigas's conjecture is not yet available, its domain of validity is fairly established.

Complementary to the universal view there is another successful contribution of the semiclassical approach to the research in quantum chaos. To every spectrum corresponding to a Hamiltonian system there are always deviations from the universal behavior, i.e., system specific features. For low-dimensional chaotic systems the later are usually nicely explained by identifying the system shortest classical periodic trajectories. For instance, knowing the actions and the stability of all periodic orbits up to a time T of a given chaotic system, the semiclassical approximation explains system specific spectral correlations within energy windows $\Delta E \geq h/T$.

The search for an universal behavior in chaotic wave functions is more elusive. In this case, one faces a different interplay between the quantum and classical scales where the system specific features become important. Actually, the investigation of nonuniversal signatures of the classical underlying dynamics in wave functions, such as scars [10], is a most fascinating subject to which several theoretical studies were devoted [11–15]. Whereas there are still several open

questions to be answered, one can naively say that it is possible to separate a "short" universal time from a "long" system specific time regime in the description of chaotic wave functions. This is, in a broad sense, the subject of the present paper.

The simplest statistical measure for chaotic wave functions fluctuations is the two-point correlation function $C(\mathbf{q}^+,\mathbf{q}^-)=\langle\psi_n(\mathbf{q}^+)\psi_n^+(\mathbf{q}^-)\rangle_\mathbf{q}$, where $\langle\cdots\rangle_\mathbf{q}$ stands for a local average in configuration space and $\psi_n(\mathbf{q})$ is the wave function of the nth energy eigenstate of a given Hamiltonian. To the best of our knowledge this autocorrelation function was first discussed by Berry [16], although admittedly very similar ideas about the characterization of chaotic wave function were already known [17,18]. Berry assumed a microcanonical probability density in the classical phase space for chaotic quantum states and obtained a simple analytical expression for $C(\mathbf{q}^+,\mathbf{q}^-)$. In line with the statistical approach, C was also reobtained by means of supersymmetric techniques in weakly disordered systems [19,20], and also by standard statistical methods [26]. The later were able to quantify the fluctuations of C around Berry's result for the mean. The correlation function C was also numerically verified by eigenfunctions studies of different dynamical systems [21–23] and experimentally observed in eigenmodes of resonating microwave cavities [24,25]. In all such studies the agreement was always very good for spatial separations up to a few wave lengths, i.e., "short" distances. By correcting C for contributions of classical trajectories for large separations $|\mathbf{q}^+-\mathbf{q}^-|$, a recent study due to Hortikar and Srednicki [27] improved Berry's formula for $C(\mathbf{q}^+,\mathbf{q}^-)$.

As a further motivation we add that the understanding of wave function correlations has some interesting direct application as, for instance, in the description of the conductance fluctuations of quantum dots in the Coulomb blockade regime [28–32]. With this background in mind, we take a fresh look into the question of eigenstates autocorrelations using the Wigner-Weyl formalism. By doing this we derive a general expression for wave function spatial correlations keeping the semiclassical approximation under strict control. We recover as limiting cases Berry's correlation function [16] as well as the aforementioned Hortikar and Srednicki result

[27]. We furthermore discuss the important role played by different kinds of averaging procedures and open a path for the inclusion of scar contributions. To make the problem tractable, we start introducing an energy smoothing, thus defining an average C. In a sense, this implies that our findings give an improved mean of the autocorrelation function C, in distinction to the treatment of fluctuations presented in [26].

The structure of the paper is as follows. In Sec. II we introduce the spectral Wigner function W, the object on which this study is built due to its simple relation to the autocorrelation function $C(\mathbf{q}^+, \mathbf{q}^-)$. There we also discuss aspects of the semiclassical approximation for W, which are essential to understand the different limiting results for $C(\mathbf{q}^+, \mathbf{q}^-)$. Section III contains the main findings of this study. We show that the semiclassical approximation for C is easier to obtain starting from a phase space representation, in particular for smooth potentials. We derive expressions for $C(\mathbf{q}^+, \mathbf{q}^-)$ depending on the averaging procedure for essentially any given spatial separation $|\mathbf{q}^+ - \mathbf{q}^-|$. In Sec. IV we relate our findings with previous analytical and numerical results discussing their validity range. We also include three appendixes. In Appendix A we show the equivalence between our expression for C with the one derived in Ref. [27] in a certain limiting regime. Appendixes B and C are technical and devoted to the demonstration of some specific formula appearing in the main text.

II. THE SPECTRAL WIGNER FUNCTION AND ITS SEMICLASSICAL APPROXIMATION

The Wigner function [33] of an individual energy eigenstate $|n\rangle$ is defined by the Weyl transformation

$$W_n(\mathbf{x}) = \int \frac{d\boldsymbol{\xi}_q}{(2\pi\hbar)^d} \psi_n(\mathbf{q}^+) \psi_n^*(\mathbf{q}^-) \exp\left(-\frac{i}{\hbar}\boldsymbol{\xi}_q \cdot \mathbf{p}\right), \quad (1)$$

where the coordinate $\boldsymbol{\xi}_q = \mathbf{q}^+ - \mathbf{q}^-$, $\mathbf{x} = (\mathbf{q}, \mathbf{p})$ is a shorthand notation for the phase space point with $\mathbf{q} = (\mathbf{q}^+ + \mathbf{q}^-)/2$ and d stands for the number of degrees of freedom of the system. From Eq. (1) it follows immediately that, upon averaging over the coordinate space $\langle \cdots \rangle_{\mathbf{q}}$, the inverse Weyl transformation of $W_n(\mathbf{x})$ gives the two-point autocorrelation function

$$C(\mathbf{q}^+, \mathbf{q}^-) \equiv \langle \psi_n(\mathbf{q}^+) \psi_n^*(\mathbf{q}^{-1}) \rangle_{\mathbf{q}}$$
$$= \int d\mathbf{p} \left\langle W_n\left(\frac{\mathbf{q}^+ + \mathbf{q}^-}{2}, \mathbf{p}\right) \right\rangle_{\mathbf{q}} \exp\left[\frac{i}{\hbar}\mathbf{p} \cdot (\mathbf{q}^+ - \mathbf{q}^-)\right].$$
$$(2)$$

Note that our definition of C is not normalized by a factor $\langle |\psi_n(\mathbf{r})|^2 \rangle_{\mathbf{q}}^{-1}$ as standard.

The essence of Berry's pioneering work [16] was to assume that the averaged Wigner function of a generic chaotic quantum state $|n\rangle$ of an autonomous system is distributed as a Dirac δ function over the surface of energy E_n, i.e., $\langle W_n(\mathbf{x}) \rangle_{\mathbf{q}} \propto \delta(H(\mathbf{x}) - E_n)$, where $H(\mathbf{x})$ is the system Hamiltonian. For a Hamiltonian of the form

$$H(\mathbf{x}) = \mathbf{p}^2/2m + V(\mathbf{q}), \quad (3)$$

this so-called microcanonical probability density in a d-dimensional configuration space leads to the well-known formula [16]

$$C(\mathbf{q}^+, \mathbf{q}^-) \propto \frac{J_{d/2-1}(p(\mathbf{q})|\mathbf{q}^+ - \mathbf{q}^-|/\hbar)}{[p(\mathbf{q})|\mathbf{q}^+ - \mathbf{q}^-|/\hbar]^{d/2-1}}, \quad (4)$$

where $p(\mathbf{q}) = \sqrt{2m[E - V(\mathbf{q})]}$, $\mathbf{q} = (\mathbf{q}^+ + \mathbf{q}^-)/2$, and $J_\nu(x)$ is the Bessel function of order ν. (The formula encountered in Ref. [16] differs from Eq. (4) by a constant due to normalization.) Since the above relation does not depend on any system specific features, scaling only with the local momentum $p(\mathbf{q})$, it directly reveals an universal behavior of chaotic wave functions. More recently, Prigodin and coworkers [19] microscopically obtained the same result for disordered systems using the nonlinear σ model, in a regime resembling to quantum chaotic systems. Impressive numerical tests of Eq. (4) were presented, for instance, in Refs. [22,23], reporting on the study of wave functions corresponding to high lying energy levels of the two-dimensional ($d=2$) conformal billiard.

In spite of the success of Eq. (4), one proviso ought to be made. Both analytical and numerical results only corroborate Berry's conjecture if one regards the average $\langle \cdots \rangle_{\mathbf{q}}$ in a broader sense. The nonlinear σ model approach averages over an ensemble of different impurities configurations. In addition to the average over $\mathbf{q} = (\mathbf{q}^+ + \mathbf{q}^-)/2$ covering regions encompassing several de Broglie wavelengths, the local averages $\langle \cdots \rangle_{\mathbf{q}}$ in Ref. [22] had to be taken over all directions of $(\mathbf{q}^+ - \mathbf{q}^-)$ for a fixed value of $|\mathbf{q}^+ - \mathbf{q}^-|$ to verify Eq. (4).

Some time ago Berry [12,34] formulated a more rigorous approach to this subject, which was recently further developed by Ozorio de Almeida [35]. It has been shown that Berry's original conjecture of microcanonical probability concentration [16] is semiclassically verified if the average runs over Wigner functions of states belonging to an energy window containing several levels [12,34,35]. This construction is best casted in terms of the spectral Wigner function, namely,

$$W(\mathbf{x}, E; \varepsilon) \equiv (2\pi\hbar)^d \sum_n \delta_\varepsilon(E - E_n) W_n(\mathbf{x}), \quad (5)$$

where the $\{E_n\}$ are the system eigenenergies. The energy smoothing function δ_ε is for convenience chosen as

$$\delta_\varepsilon(E - E_n) = \frac{\varepsilon/\pi}{(E - E_n)^2 + \varepsilon^2}, \quad (6)$$

in correspondence to an energy window of width ε centered at E. Likewise, we introduce the smoothed eigenstate autocorrelation function

$$C_\varepsilon(\mathbf{q}^+, \mathbf{q}^-, E) = \Delta \sum_n \delta_\varepsilon(E - E_n) \psi_n(\mathbf{q}^+) \psi_n^*(\mathbf{q}^-), \quad (7)$$

where Δ is the mean level density at energy E, defined as $\Delta \equiv \langle \Sigma_n \delta_\varepsilon(E - E_n) \rangle_\varepsilon^{-1}$, with the average taken over the energy levels contained by the energy window ε centered at E. (When using the semiclassical approximation, for the sake of consistency, Δ is obtained from the Weyl energy level density, i.e., $\Delta \equiv 1/\rho_W$.) As follows from Eq. (1), the inverse of W_n directly gives $\psi_n(\mathbf{q}^+)\psi_n^*(\mathbf{q}^-)$ rendering

$$C_\varepsilon(\mathbf{q}^+, \mathbf{q}^-, E) = \Delta \int \frac{d\mathbf{p}}{(2\pi\hbar)^d} W\left(\frac{\mathbf{q}^+ + \mathbf{q}^-}{2}, \mathbf{p}, E; \varepsilon\right)$$

$$\times \exp\left[\frac{i}{\hbar} \mathbf{p} \cdot (\mathbf{q}^+ - \mathbf{q}^-)\right]. \quad (8)$$

The advantage of using W is that it provides ways for amenable semiclassical approximations in different energy smoothing regimes, allowing for the analysis of C_ε at any given spatial scale separation. Equation (8) is the starting point of all results derived in this paper. The remaining part of this section is devoted to the presentation of the limiting approximations to W based on the semiclassical picture of chord and centers, postponing to the forthcoming section the corresponding analysis of $C_\varepsilon(\mathbf{q}^+, \mathbf{q}^-, E)$.

A. The semiclassical spectral Wigner function

The spectral Wigner function is related to the Weyl propagator $U_t(\mathbf{x})$, i.e., the Weyl transform of the propagator $\langle \mathbf{q}^+ | \exp(-it\hat{H}/\hbar) | \mathbf{q}^- \rangle$, through [12,35]

$$W(\mathbf{x}, E; \varepsilon) = \frac{1}{\pi\hbar} \mathrm{Re} \int_0^\infty dt \, e^{-\varepsilon t/\hbar} U_t(\mathbf{x}) \exp\left(\frac{i}{\hbar} E t\right). \quad (9)$$

The semiclassical approximation of W is directly obtained by inserting in the above equation the semiclassical expression for the Weyl propagator [35], namely,

$$U_t^{\mathrm{sc}}(\mathbf{x}) = \sum_j \frac{2^d}{|\det[\mathbb{1} + \mathcal{M}_j(\mathbf{x},t)]|^{1/2}} \exp\left[i\frac{S_j(\mathbf{x},t)}{\hbar} + i\beta_j\right]. \quad (10)$$

Here the sum is taken over all classical trajectories with the same traversal time t whose phase space end points $\mathbf{x}_j^\pm$ are joined by a chord $\xi_j(\mathbf{x}) = \mathbf{x}_j^+ - \mathbf{x}_j^-$ centered at $\mathbf{x}$. Figure 1 illustrates the phase space structure beneath the semiclassical Weyl propagator. The Maslov phase associated with the jth classical trajectory is given by β_j. In Eq. (10), $\mathbb{1}$ is the identity and $\mathcal{M}_j$ is the symplectic matrix (or stability matrix). The latter corresponds to the map $\delta \mathbf{x}_j^+ = \mathcal{M}_j \delta \mathbf{x}_j^-$, resulting from the linearization of the dynamics in the neighborhood of $\mathbf{x}_j^\pm$. The symbol $S_j(\mathbf{x},t)$ stands for the action, also called *center action* [35], given by

$$S_j(\mathbf{x},t) = \oint_i d\mathbf{q} \cdot \mathbf{p} - \int dt \, H_W[\mathbf{x}_j(t)], \quad (11)$$

where H_W is the Weyl Hamiltonian, i.e., the Weyl symbol of the Hamiltonian operator. It is worth recalling that the Weyl Hamiltonian $H_W(\mathbf{x})$ only coincides with the classical one
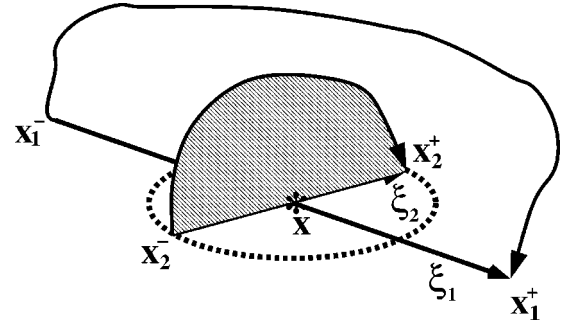

FIG. 1. Chord structure of the semiclassical Weyl propagator, Eq. (10), and of the spectral Wigner function Eq. (13) in a $2d$-dimensional phase space. For a central point $\mathbf{x}$ we show typical chords with their tips connected by classical trajectories on different energy shells but with the same traversal time t. The dashed line indicates the locus, on a given energy shell E, of all the tips of chords centered at $\mathbf{x}$. The classical trajectories connecting these types of chords are the semiclassical contributions to W. The dashed area represents the symplectic area corresponding to the action $S_2(\mathbf{x},E)$ (see text).

$H_W(x)$, when the latter is of the form given by Eq. (3). The first integral at the right-hand side rhs of Eq. (11) is the symplectic area enclosed by the circuit taken along the jth trajectory connecting $\mathbf{x}_j^-$ to $\mathbf{x}_j^+$ and closed by the chord $-\xi_j(\mathbf{x})$ (see Fig. 1). For autonomous systems the second integral is simply the product of the energy E_j corresponding to the jth trajectory, with its traversal time t_j. The variation of S_j with respect to the independent variables [35] leads to

$$\xi_{j\mathbf{q}} = -\partial_j/\partial \mathbf{p}, \quad \xi_{jp} = \partial S_j/\partial \mathbf{q}, \quad \text{and} \quad -E_j = \partial S_j/\partial t. \quad (12)$$

At sufficiently short times for each phase space point $\mathbf{x}$ there is only one small chord contributing to the sum in Eq. (10). The short trajectory connecting the chord end points has a Maslov phase $\beta_0 = 0$. In distinction, as t is increased, due to bifurcations there is a proliferation of different chords to be summed in Eq. (10).

The starting point for the semiclassical analysis of W is encountered by replacing Eq. (10) into Eq. (9)

$$W(\mathbf{x}, E; \varepsilon) = \frac{2^{d+1}}{2\pi\hbar} \mathrm{Re} \sum_j \int_0^\infty dt \frac{e^{-\varepsilon t/\hbar}}{|\det[\mathbb{1} + \mathcal{M}_j(\mathbf{x},t)]|^{1/2}}$$

$$\times \exp\left\{\frac{i}{\hbar}[S_j(\mathbf{x},t) + Et] + i\beta_j\right\}. \quad (13)$$

This formula exemplifies the general structure of the semiclassical Weyl representation of any quantum object as being given in terms of its classical chord structure in phase space. In general, this fact is revealed by the use of the stationary phase approximation to obtain the dominant contributions for any observable. This premise will guide our analysis of C_ε in the following section. In the following, we show how the stationary phase method works in the case of the spectral Wigner function given by Eq. (13).

The points of stationary phase are the solutions of

$$\frac{d}{dt}[S_j(\mathbf{x},t)+Et]=0. \tag{14}$$

This equation fixes the traveling time along the jth trajectory $t_j(E)$ at the energy E, for which

$$S_j(\mathbf{x},t_j)+Et_j(E)=S_j(\mathbf{x},E), \tag{15}$$

where the action $S_j(\mathbf{x},E)$ is the symplectic area corresponding to the first integral at the rhs of Eq. (11), with the momentum $|\mathbf{p}|$ fixed by the energy E. In other words, the stationary phase condition selects those trajectory segments that belong to a single energy shell $\mathcal{C}$. Thus, for such trajectories, all the chords centered at $\mathbf{x}$ have their tips on $\mathcal{C}$. If all the stationary points $t_j(E)$ are isolated, which is generally the case when the chords centered at $\mathbf{x}$ are sufficiently separated, we can evaluate W by stationary phase [35], that yields

$$W(\mathbf{x},E;\varepsilon)=\frac{2^{d+1}}{\sqrt{2\pi\hbar}}\sum_j e^{-\varepsilon t_j/\hbar}A_j(\mathbf{x},E)\cos\left[\frac{S_j(\mathbf{x},E)}{\hbar}+\gamma_j\right], \tag{16}$$

where the amplitude is explicitly written as

$$A_j(\mathbf{x},E)=\left|\frac{dt_j}{dE}\det\{\mathbb{1}+\mathcal{M}_j(\mathbf{x},t_j(E))\}^{-1}\right|^{1/2}, \tag{17}$$

and we collected the Maslov phases of the classical contributions in γ_j. If the energy shell $\mathcal{C}$ is closed and convex and $\mathbf{x}$ lies inside it there will be always contributing chords to Eq. (16). To keep the presentation simple we shall only consider convex energy shells in this paper.

B. The role of the energy average

The smoothing ε parameter plays an essential role in regulating the convergence of the semiclassical approximation for the spectral Wigner function W: as ε becomes smaller, longer classical paths start contributing relevantly to the sum in Eq. (16). It is customary to define two characteristic semiclassical scales for ε [12,34]. The first one is the outer scale $\varepsilon_{\text{large}}\equiv\hbar/\tau_{\text{min}}$, where τ_{min} is the period of the shortest periodic orbit, characterizing the typical time to flow around the energy shell. The second one is the inner scale $\varepsilon_{\text{small}}\equiv\hbar/\tau_{\text{H}}$, where τ_{H} is the Heisenberg time defined by the mean level spacing Δ in the considered energy window as $\tau_{\text{H}}=\hbar/\Delta$.

Particularly strong contributions to W arise when $\mathbf{x}$ is taken in the neighborhood of caustics. At such singular points the standard stationary phase approximation is bound to fail. When the evaluating point $\mathbf{x}$ approaches a caustic of the integrand in Eq. (13), generically two or more stationary phase points $t_j(E)$ coalesce and so do the corresponding chords $\xi_j(\mathbf{x})$. Therefore, we shall also often speak of coalescing chords at caustics. The most important kind of caustics influencing C_ε will be those at the energy shell itself and the ones near periodic orbits on $\mathcal{C}$. As we will show, the first ones are associated with short times, whereas the others are associated with the long time dynamics. Correspondingly we distinguish two energy averaging regimes in W for points $\mathbf{x}$

near the energy shell: (a) $\varepsilon\gg\varepsilon_{\text{large}}$ when the signatures of all the long trajectories are suppressed and (b) the opposite situation when $\varepsilon<\varepsilon_{\text{large}}$ and more trajectories do contribute. Here, to keep the approximation under control, $\varepsilon\gg\varepsilon_{\text{small}}$ is required.

Let us first consider the case when $\varepsilon\gg\varepsilon_{\text{large}}$. Here, only one short classical trajectory, with traversal time t_0 fixed by the stationary phase condition, contributes to W [35]. The shorter chord in Fig. 1 serves to illustrate this situation. As $\mathbf{x}\to\mathcal{C}$, t_0 approaches the lower integration limit in Eq. (13) spoiling the stationary phase approximation. This difficulty can be circumvented in the following way. Since the action $S(\mathbf{x},t)$ is always an odd function of t and by changing the cutoff function, $\exp(-\varepsilon t/\hbar)$, for an even one with respect to t, we write Eq. (13) as

$$W(\mathbf{x},E;\varepsilon)\simeq\frac{2^d}{2\pi\hbar}\int_{-\infty}^{\infty}dt\,\frac{e^{-\varepsilon|t|/\hbar}}{|\det[\mathbb{1}+\mathcal{M}_0(\mathbf{x},t)]|^{1/2}}$$

$$\times\exp\left\{\frac{i}{\hbar}[S_0(\mathbf{x},t)+Et]\right\}. \tag{18}$$

The resulting integrand displays two stationary phase points located at $\pm t_0$ that coalesce at $t=0$ as $\mathbf{x}$ approaches $\mathcal{C}$. The structure of coalescing stationary points at the origin can be obtained by expanding the center action up to third order in t [35]

$$S(\mathbf{x},t)\approx-tH_W(\mathbf{x})-\tfrac{1}{24}t^3\dot{\mathbf{x}}\mathcal{H}\dot{\mathbf{x}}, \tag{19}$$

where $\dot{\mathbf{x}}$ is the phase space velocity and $\mathcal{H}$ the Hessian matrix of the Weyl Hamiltonian, both taken at the phase space point $\mathbf{x}$. The integral in Eq. (18) can now be evaluated by the uniform approximation method [36] by invoking a suitable change of the integration variable. Such transformation, $z\equiv z(t)$, is the one that reduces the integrand phase in Eq. (18) to the canonical form $z^3/3-\gamma^2 z$ (see, for instance, Ref. [37]). Mapping the stationary points $\pm t_0$ into the new ones in z, yields to $\gamma=-[3S(\mathbf{x},E)/2]^{1/3}$. Thus, we obtain

$$W(\mathbf{x},E;\varepsilon)=\frac{2^{d+1}}{\sqrt{2\hbar}}e^{-\varepsilon|t_0|/\hbar}A_0(\mathbf{x},E)\left[\frac{3S_0(\mathbf{x},E)}{2\hbar}\right]^{1/6}$$

$$\times\text{Ai}\left(-\left(\frac{3S_0(\mathbf{x},E)}{2\hbar}\right)^{2/3}\right), \tag{20}$$

where $\text{Ai}(y)$ is the Airy function [38]. This result corrects for a small mistake in Eq. (7.20) of Ref. [35]. It also contains the relation previously discussed for $\mathbf{x}$ taken deep inside the energy shell. As the evaluation point $\mathbf{x}$ recedes from $\mathcal{C}$, the Airy function argument (in modulus) grows very fast. Hence, we are entitled to employ the Airy function approximation for large negative arguments and retrieve Eq. (16), provided that for the short trajectory $\gamma_0=0$.

As $\mathbf{x}$ further approaches the energy shell $\mathcal{C}$, the spectral Wigner function becomes very simple (provided $\varepsilon\gg\varepsilon_{\text{large}}$). In such situation there is an apparent indeterminacy in the amplitude of Eq. (20) since the symplectic area $S(\mathbf{x},E)$ vanishes and the amplitude $A_0(\mathbf{x},E)$ diverges. In this case it is

an accurate approximation to represent the short trajectory by the short chord $\boldsymbol{\xi}_0 \approx t_0 \dot{\mathbf{x}}$, and hence the stability matrix $\mathcal{M}_0$ becomes the identity. Thus

$$S_0(\mathbf{x},E) \simeq \tfrac{1}{12} t_0^3 \dot{\mathbf{x}} \mathcal{H}_0 \dot{\mathbf{x}} = \tfrac{4}{3}\sqrt{2} \frac{[E-H_W(\mathbf{x})]^{3/2}}{(\dot{\mathbf{x}}\mathcal{H}_0\dot{\mathbf{x}})^{1/2}}, \qquad (21)$$

and

$$\left| \frac{dt_0}{dE} \right|^{1/2} = \left(\frac{t_0}{2} \left| \dot{\mathbf{x}} \mathcal{H} \dot{\mathbf{x}} \right| \right)^{-1/2}. \qquad (22)$$

Hence, as it was already shown [39,35]

$$W(\mathbf{x},E;\varepsilon) \xrightarrow[\mathbf{x} \to \mathcal{C}]{} \frac{2}{|\hbar^2 \dot{\mathbf{x}} \mathcal{H}_0 \dot{\mathbf{x}}|^{1/3}} \mathrm{Ai}\left(\frac{2[H_W(\mathbf{x})-E]}{(\hbar^2\dot{\mathbf{x}}\mathcal{H}_0\dot{\mathbf{x}})^{1/3}} \right). \qquad (23)$$

In this situation, $\mathbf{x} \to \mathcal{C}$ and $\varepsilon \gg \varepsilon_{\mathrm{large}}$, for the strict semiclassical regime we easily recover the microcanonical probability distribution

$$W(\mathbf{x},E;\varepsilon) \approx \delta(H_W(\mathbf{x})-E), \qquad (24)$$

by recalling that $\lim_{\alpha \to 0} \alpha^{-1} \mathrm{Ai}(\mathbf{y}/\alpha) = \delta(\mathbf{y})$. This result does not come as a surprise, it is just telling us that we washed out most quantum interference effects reaching the classical limit while taking $\varepsilon \gg \varepsilon_{\mathrm{large}}$. It is only by narrowing ε that one can explore the rich structure of the spectral Wigner function and unveil nontrivial quantum features. This discussion shall be resumed in a deeper level in the following section, but we can already anticipate that Eq. (24) is remarkably robust.

Let us discuss now the case where $\varepsilon < \varepsilon_{\mathrm{large}}$ and $\mathbf{x}$ is taken close to the energy shell $\mathcal{C}$. Here, one also has to account for pairs of coalescing chords in Eq. (13), schematically shown in Fig. 2. These are the short chords corresponding to long trajectories orbiting between its tips and winding very closely to a periodic orbit. When $\mathbf{x} \to \mathcal{C}$ their traversal times and actions, $S(\mathbf{x},E)$, become degenerate with those of the corresponding periodic orbit. Thus, Eq. (20) has to be corrected by adding the so-called scar contributions to the spectral Wigner function, first developed by Berry [12] and latter refined by Ozorio de Almeida [35]. The latter formula describes the Wigner scars as a peak of extra intensity along the periodic orbits on the energy shell decorated with a fringe pattern. As it was shown in Ref. [15] such Wigner scars extend deep inside the energy shell where the spectral Wigner function is semiclassically given by Eq. (16) for any arbitrary value of ε. Indeed, when the action of a periodic orbit is Bohr quantized the contributions of trajectory segments for chords whose tips lie on the periodic orbit, can be added in phase to Eq. (16). Hence the Wigner scars have an enhanced pattern of concentric rings of oscillatory amplitude on a two-dimensional surface defined by the centers of all the chords with end point on the periodic orbit [15]. Only the edge of this surface corresponds to the domain of the Berry's scars formula. This shows that the semiclassical spectral Wigner function is in general not restricted to the energy shell, and thus to short chord contributions. In other words, we say that the old microcanonical conjecture of Voros and
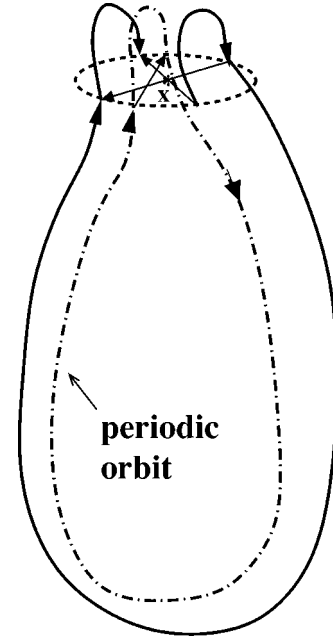

FIG. 2. Illustration of a composition of trajectory segments that closely follow a periodic orbit. Berry's scar formula singles out the trajectories connecting the tips of the two depicted chords that become indistinguishable from the period orbit as $\mathbf{x}$ approaches C.

Berry [18,16], has important semiclassical corrections. The distinction between contributions of the large and short chords will appear again in the study of the spectral autocorrelation function C_ε in the following section.

III. CORRELATIONS OF ERGODIC WAVE FUNCTIONS FOR DIFFERENT ENERGY AVERAGING REGIMES

In this section we derive a general semiclassical formula for $C_\varepsilon(\mathbf{q}^+, \mathbf{q}^-, E)$ expressed in terms of the system classical chord structure. Our analysis is build on the semiclassical approximations for the spectral Wigner function W presented in the foregoing section.

For any given pair of points in position space, $\mathbf{q}^+$ and $\mathbf{q}^-$, the integral in Eq. (8) is performed over the entire d-dimensional momentum space. In this study we only consider $\mathbf{q}^+$ and $\mathbf{q}^-$ within classically allowed regions. Hence, the integration momentum space intercepts the energy shell and is naturally divided into a domain located in the interior of $\mathcal{C}$ and another at its exterior. This is illustrated in Fig. 3. For convex energy surfaces, the ones considered here, the spectral Wigner function, whose argument is $\mathbf{q}=(\mathbf{q}^+ +\mathbf{q}^-)/2$, exponentially vanishes for values of $\mathbf{p}$ in the phase space region exterior to $\mathcal{C}$. Hence, in general, the main contribution to the integral in Eq. (8) arises from momenta in the interior of $\mathcal{C}$ and at its immediate neighborhood. Thus, we are allowed to bound the effective momentum integration space in Eq. (8) to the classically allowed momenta. We name the so defined integration space the "momentum space associated to $\mathbf{q}=(\mathbf{q}^+ + \mathbf{q}^-)/2$."

In line with Sec. II, first we find the general chord structure that C_ε inherits from W. This is done by inserting into Eq. (8) the semiclassical expression for the spectral Wigner
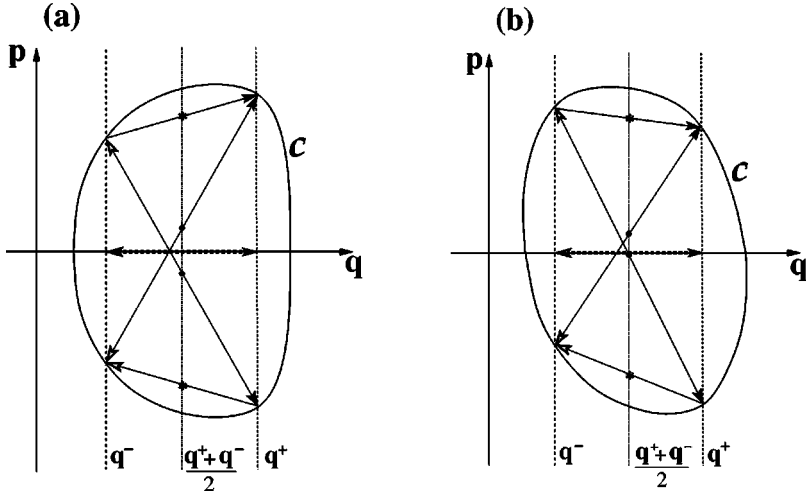
(a)

(b)

FIG. 3. Chord structure of the semiclassical approximation for the spectral autocorrelation function C_ε. The horizontal dashed lines represent the projection on configuration space of the chords $\xi_\mathbf{q}$ matching the vectors $\pm(\mathbf{q}^+ - \mathbf{q}^-)$. The points of stationary phase are located on the d-dimensional associated momentum space to $\mathbf{q} = (\mathbf{q}^+ + \mathbf{q}^-)/2$ and indicated by asterisks ($*$) and dots ($\bullet$) (see text for details). $\mathcal{C}$ stands for the $(2d-1)$-dimensional surface of constant energy E whereas the axis $\mathbf{q}$ and $\mathbf{p}$ represent d-dimensional surfaces. The semiclassical contributions to C_ε are given by all trajectories on $\mathcal{C}$ flowing between the tips of chords $\xi_\mathbf{q}$. Panel (a) illustrates a typical time reversal symmetric case, while (b) a case when this symmetry is absent.

function given by Eq. (16), which is valid for any arbitrary ε. The resulting integral can be casted as

$$C_\varepsilon(\mathbf{q}^+, \mathbf{q}^-, E) = \Delta \sum_j \frac{e^{-\varepsilon t_j/\hbar}}{(2\pi\hbar)^{d+1/2}} [I_j^+(\mathbf{q}^+, \mathbf{q}^-, \mathbf{E}) e^{i\gamma_j}$$

$$+ I_j^-(\mathbf{q}^+, \mathbf{q}^-, E) e^{-i\gamma_j}], \qquad (25)$$

with

$$I_j^\pm = 2^d \int d\mathbf{p} A_j(\mathbf{x}, E) \exp\left\{\frac{i}{\hbar}[S_j(\mathbf{x}, E) \pm \mathbf{p}\cdot(\mathbf{q}^+ - \mathbf{q}^-)]\right\}. \qquad (26)$$

Now we evaluate $I_j^\pm$ by stationary phase. The stationary phase points $\mathbf{p}_j \equiv \mathbf{p}_j(\mathbf{q}^+, \mathbf{q}^-, E)$ are solutions of

$$\frac{\partial}{\partial\mathbf{p}}\left[S_j\left(\frac{\mathbf{q}^+ + \mathbf{q}^-}{2}, \mathbf{p}, E\right)\right] = \pm(\mathbf{q}^+ - \mathbf{q}^-) \qquad (27)$$

for $I_j^\pm$. We recall that the variation of $S_j(\mathbf{x}, E)$ with respect to the independent variables $\mathbf{q}$ and $\mathbf{p}$ are given in Eq. (12). Hence, the first member of Eq. (27) is exactly $-\xi_{j\mathbf{q}} = -(\mathbf{q}_j^+ - \mathbf{q}_j^-)$. In other words, the stationary phase condition selects those classical j trajectories in the energy shell whose projected chords in the configuration space match the vectors $\pm(\mathbf{q}^+ - \mathbf{q}^-)$. This geometrical structure is sketched in Fig. 3, where the projected chords are indicated by dashed vectors. In the same figure, the classical j trajectories are those flowing between the intersections of the momentum spaces corresponding to $\mathbf{q} = \mathbf{q}^-$ and $\mathbf{q} = \mathbf{q}^+$ with the energy surface $\mathcal{C}$. The panel (a) of Fig. 3 corresponds to time reversal symmetric flows, whereas (b) represents the cases when this symmetry is absent. The locations of the many possible stationary phase points $\mathbf{p}_j$ in the momentum space associated to $\mathbf{q} = (\mathbf{q}^+ + \mathbf{q}^-)/2$ are indicated by dots and asterisks. While for $\mathbf{q}^- \to \mathbf{q}^+$ the chords centered at "asterisks" coalesce to a zero length chord at the energy shell $\mathcal{C}$, the ones centered at "dots" are typically large. This allow us to name the chords centered at "asterisks" as "short" chords and the ones centered at "dots" as "long" chords.

Provided that the stationary points $\mathbf{p}_j$ are sufficiently far apart from each other, we can safely evaluate I_j^+ and I_j^- by the stationary phase method. The latter requires a symmetrized Legendre transformation in the phases of Eq. (26), which is conveniently expressed by the standard textbook action S [35], with variables in the configuration space, namely,

$$S_j(\mathbf{q}^\pm, \mathbf{q}^\mp, E) = S_j(\mathbf{x}_j, E) \pm \mathbf{p}_j \cdot (\mathbf{q}^\pm - \mathbf{q}^\mp), \qquad (28)$$

where $\mathbf{x}_j = (\mathbf{q}, \mathbf{p}_j)$ with $\mathbf{q} = (\mathbf{q}^+ + \mathbf{q}^-)/2$ and $\mathbf{p}_j \equiv \mathbf{p}_j(\mathbf{q}^+, \mathbf{q}^-, E)$. We obtain for the nonoscillatory factor of both I_j^+ and I_j^-

$$2^d A_j(\mathbf{x}_j, E)\left|\det\left(\frac{\partial^2 S_j(\mathbf{x}, E)}{\partial\mathbf{p}^2}\right)\right|^{-1/2}\bigg|_{\mathbf{x}=\mathbf{x}_j} = |D_j|^{1/2}, \quad (29)$$

where

$$D(\mathbf{q}^+, \mathbf{q}^-, E) \equiv (-1)^d \det\begin{pmatrix} \dfrac{\partial^2 S}{\partial\mathbf{q}^- \partial\mathbf{q}^+} & \dfrac{\partial^2 S}{\partial\mathbf{q}^- \partial E} \\[2ex] \dfrac{\partial^2 S}{\partial\mathbf{q}^+ \partial E} & \dfrac{\partial^2 S}{\partial E^2} \end{pmatrix}. \qquad (30)$$

The details of the derivation leading to Eq. (29) can be found in Appendix A.

For time-reversal invariant systems, to every j trajectory on $\mathcal{C}$ going from $\mathbf{q}^-$ to $\mathbf{q}^+$ (solution of the integral I_j^+) there is a corresponding time reversed pair going from $\mathbf{q}^+$ to $\mathbf{q}^-$ (solution of the integral I_j^-). Evidently both terms contribute with the same stationary phase and amplitude to the sum in Eq. (25). Hence

$$C_\varepsilon(\mathbf{q}^+, \mathbf{q}^-, E) \approx \frac{2\Delta}{(2\pi\hbar)^{(d+1)/2}} \sum_j e^{-\varepsilon t_j/\hbar} |D_j(\mathbf{q}^+, \mathbf{q}^-, E)|^{1/2}$$

$$\times \cos\left[\frac{S_j(\mathbf{q}^+, \mathbf{q}^-, E)}{\hbar} + \gamma_j + \nu_j\frac{\pi}{4}\right], \qquad (31)$$

where $\nu_j \equiv \mathrm{sgn}[\partial^2 S_j(\mathbf{x},E)/\partial \mathbf{p}^2]$. This is essentially the main finding of Ref. [27].

Let us now discuss the conditions under which Eq. (31) fails. When $\mathbf{q}^-$ approaches $\mathbf{q}^+$, the points $\mathbf{x}_j$, represented by asterisks in Fig. 3, move closer to the energy shell. As we learned in Sec. II this is a case where the semiclassical approximation for the spectral Wigner function, from which Eq. (31) was obtained, fails. Remarkably, even in this limit where $\mathbf{q}^- \to \mathbf{q}^+$ there are "long" chords whose center points $\mathbf{x}_j$, indicated by dots in Fig. 3, are typically far from $\mathcal{C}$. Such contributions to C_ε are still well described by Eq. (31), but are obviously unrelated to the "short" chords. The approximation scheme for W developed in the preceding section to deal with the classical contributions due to the "short" chords centered at points $\mathbf{x}_j$ close to $\mathcal{C}$, can be also used to obtain C_ε. In the remainder of this section we pursue this path for two very different energy smoothing regimes and obtain a semiclassical approximation of C_ε valid for any spatial separation scale within the classical allowed region.

At this point an important remark is in order. The chord structure for a fixed distance $|\mathbf{q}^+ - \mathbf{q}^-|$ sketched in Fig. 3 is robust upon changes of $\mathbf{q} = (\mathbf{q}^+ + \mathbf{q}^-)/2$ unless one of the points $\mathbf{q}^\pm$ reaches the boundary of the classical allowed region. When this condition is met, the "short" chords coalesce with the "long" ones, corresponding in Eq. (25) to the case of coalescing stationary points. A semiclassical investigation for a similar situation has already been reported [39], but it did not address wave function correlations. This is a most interesting physical situation owing to its relation to tunneling rates and possible implications to the already mentioned Coulomb blockade systems [28–32]. Unfortunately we were not able to develop a semiclassical approximation to this problem yet. We avoid it in this paper by restricting our analysis to points $\mathbf{q}^\pm$ inside the classical allowed region and distant from its boundary by a couple of de Broglie wavelengths.

A. Large $\varepsilon \gg \varepsilon_{\mathrm{large}}$ smoothing regime

For $\varepsilon \gg \varepsilon_{\mathrm{large}}$ the cutoff parameter ε suppresses all but the shortest trajectory contribution to Eq. (31). The latter connects both tips of a "short" chord $\boldsymbol{\xi}_0$ (see Fig. 3). As discussed before, when the center $\mathbf{x}_0$ of $\boldsymbol{\xi}_0$ approaches the energy shell $\mathcal{C}$, we have to employ the corresponding uniform approximation to W, given by Eq. (20).

Instead of directly Fourier transforming the semiclassical spectral Wigner function, it is advantageous to step back, use W as given by Eq. (18), and invert the integration order. That is

$$C_\varepsilon(\mathbf{q}^+,\mathbf{q}^-,E) \simeq \frac{\Delta}{2\pi\hbar} \int_{-\infty}^\infty dt\, e^{-\varepsilon|t|/\hbar} F_0(\mathbf{q}^+,\mathbf{q}^-,t)$$

$$\times \exp\left(\frac{iEt}{\hbar}\right), \qquad (32)$$

where

$$F_0(\mathbf{q}^+,\mathbf{q}^-,t) \equiv \frac{2^d}{(2\pi\hbar)^d} \int d\mathbf{p}\, \frac{1}{|\det[\mathbb{1}+\mathcal{M}_0(\mathbf{x},t)]|^{1/2}}$$

$$\times \exp\left\{ \frac{i}{\hbar}[S_0(\mathbf{x},t)+\mathbf{p}\cdot(\mathbf{q}^+-\mathbf{q}^-)]\right\}. \qquad (33)$$

The above integral is evaluated by the stationary phase method. The stationary phase point $\mathbf{p}_0 \equiv \mathbf{p}_0(\mathbf{q}^+,\mathbf{q}^-,t)$ is the solution of

$$-\boldsymbol{\xi}_{0\mathbf{q}} \equiv \frac{\partial}{\partial\mathbf{p}}\left[S_0\left(\frac{\mathbf{q}^+ + \mathbf{q}^-}{2},\mathbf{p},t\right)\right] = -(\mathbf{q}^+-\mathbf{q}^-). \qquad (34)$$

In analogy to the case that leads to Eq. (28), the phase factor is best written in terms of the standard textbook action R, with variables in the configuration space, namely,

$$R_0(\mathbf{q}^+,\mathbf{q}^-,t) = S_0(\mathbf{x}_0,t) + \mathbf{p}_0 \cdot (\mathbf{q}^+-\mathbf{q}^-). \qquad (35)$$

Substituting the obtained stationary phase approximation of F_0 into Eq. (32) we write C_ε as

$$C_\varepsilon(\mathbf{q}^+,\mathbf{q}^-,E) \simeq \frac{\Delta}{(2\pi\hbar)^{d/2+1}} \int_{-\infty}^\infty dt\, g(t)$$

$$\times \exp\left[\frac{i}{\hbar}\Phi(t,\theta)+i\nu_0(t)\frac{\pi}{4}\right], \qquad (36)$$

where $\nu_0(t) \equiv \mathrm{sgn}[\partial^2 S_0(\mathbf{x},t)/\partial\mathbf{p}^2]$. The function $g(t)$ gives the amplitude

$$g(t) = 2^d e^{-\varepsilon|t|/\hbar} \left| \det[\mathbb{1}+\mathcal{M}_0(\mathbf{x},t)]\det\left(\frac{\partial^2 S_0(\mathbf{x},t)}{\partial\mathbf{p}^2}\right)\right|^{-1/2}\Bigg|_{\mathbf{x}=\mathbf{x}_0}, \qquad (37)$$

with $\mathbf{x}_0 = (\mathbf{q},\mathbf{p}_0)$, $\mathbf{q} = (\mathbf{q}^+ + \mathbf{q}^-)/2$, and $\mathbf{p}_0 \equiv \mathbf{p}_0(\mathbf{q}^+,\mathbf{q}^-,t)$. The phase Φ stands for

$$\Phi(t,\theta) = R_0(\mathbf{q}^+,\mathbf{q}^-,t) + Et, \qquad (38)$$

where we introduced $\theta \propto |\mathbf{q}^+ - \mathbf{q}^-|$ as a control parameter of the integral, i.e., $\mathbf{x}_0 \to \mathcal{C}$ when $\theta \to 0$.

The integral in Eq. (36) is dominated by the stationary phase points located at $\pm t_0(\theta,E)$ corresponding to the traversal time of the shortest trajectory going from $\mathbf{q}^-$ to $\mathbf{q}^+$ and the one running backwards in time. As $\theta \to 0$, $\pm t_0(\theta,E)$ coalesce at the origin. This situation again is very similar to the one encountered in the preceding section when dealing with the spectral Wigner function for $\mathbf{x}$ near the energy shell [i.e., the one that leads to Eq. (20)]. The difference is in the functional form of the phase Φ and on the behavior of $g(t)$ near the origin. For a Hamiltonian of the form Eq. (3) we show in Appendix B that both the phase Φ and the amplitude $g(t)$ have a singularity at the origin. Notwithstanding, the integral in Eq. (36) is finite and can be evaluated using the uniform approximation method [37]. The result is

$$C_\varepsilon(\mathbf{q}^+,\mathbf{q}^-,E) = \frac{2\pi\Delta}{(2\pi\hbar)^{(d/2)+1}}[|D_0(\mathbf{q}^+,\mathbf{q}^-,E)|$$

$$\times S_0(\mathbf{q}^+,\mathbf{q},E)]^{1/2}J_{d/2-1}\left(\frac{S_0(\mathbf{q}^+,\mathbf{q}^-,E)}{\hbar}\right),$$

(39)

where we left out the smoothing factor $e^{-\varepsilon|t_0|/\hbar}$, since for practical purposes the condition $t_0 \ll \hbar/\varepsilon$ is always met. Details about the evaluation of the integral in Eq. (36) leading to Eq. (39) are found in Appendix B, where we explicitly use H in the form given by Eq. (3).

The above semiclassical approximation for $C_\varepsilon(\mathbf{q}^+,\mathbf{q}^-,E)$ is valid for any separation $|\mathbf{q}^+-\mathbf{q}^-|$, provided the arguments belong to the classical allowed region. Let us examine the small and large separation limits. As $\mathbf{q}^- \to \mathbf{q}^+$ the shortest trajectory on $\mathcal{C}$ is well approximated by the "short" chord $\boldsymbol{\xi}_0$, and the action S_0 turns into

$$S_0(\mathbf{q}^+,\mathbf{q}^-,E) \approx p_0(\mathbf{q})|\mathbf{q}^+-\mathbf{q}^-|,$$

(40)

where $p_0(\mathbf{q}) = \sqrt{2m[E-V(\mathbf{q})]}$. Hence, the determinant D_0 simplifies to

$$|D_0(\mathbf{q}^+,\mathbf{q}^-,E)|^{1/2} \approx m\frac{p_0(\mathbf{q})^{(d-3)/2}}{|\mathbf{q}^+-\mathbf{q}^-|^{(d-1)/2}}.$$

(41)

[The derivation of Eqs. (40) and (41) is found in Appendix C.] Collecting the results, we write

$$C(\mathbf{q}^+,\mathbf{q}^-) = \frac{(2\pi)^{d/2}mp(\mathbf{q})^{d-2}}{(2\pi\hbar)^d\rho_w(E)}\frac{J_{d/2-1}(p(\mathbf{q})|\mathbf{q}^+-\mathbf{q}^-|/\hbar)}{[p(\mathbf{q})|\mathbf{q}^+-\mathbf{q}^-|/\hbar]^{d/2-1}}$$

(42)

and recover, by an appropriate normalization, Berry's original result Eq. (4). In the corresponding opposite limit, when $|\mathbf{q}^+-\mathbf{q}^-|$ is large, we use the asymptotic expansion of the Bessel function for large arguments, namely, $J_\nu(x) \approx \sqrt{2/(\pi x)}\cos(x-\nu\pi/2-\pi/4)$ and retrieve the semiclassical approximation given by Eq. (31) for the shortest trajectory.

B. Small $\varepsilon < \varepsilon_{\text{large}}$ smoothing regime

As the smoothing parameter ε is shrinked, longer trajectories have to be taken into account. As a consequence, when $\varepsilon < \varepsilon_{\text{large}}$, the approximation scheme becomes subtler than the simplified one discussed in Sec. III A. Before exploring this regime, it is useful to remind ourselves that the semiclassical contributions to the spectral Wigner function come from orbits connecting the tips of either "short" or "long" chords, as depicted in Fig. 3. We thus classify the classical trajectories into three categories.
(a) Trajectories connecting tips of "long" chords. We already discussed this case at the beginning of Sec. III. Here, since the trajectories are isolated, we just use Eq. (31). Difficulties, if any, arise from the large number of trajectories entering the sum, as regulated by the ε.
(b) Short trajectories connecting "short" chords." These were analyzed in Sec. III A.

(c) Long trajectories connecting "short chords." The analysis of $C_\varepsilon(\mathbf{q}^+,\mathbf{q}^-,E)$ becomes much clearer in the two cases namely, $\mathbf{x}$ close and far from the energy surface $\mathcal{C}$, discussed in the following.

When the long trajectories have tips on "short" chords, and $\mathbf{q}^-$ approaches $\mathbf{q}^+$, the centers $\mathbf{x}_j$ of these chords approach $\mathcal{C}$. Here in addition to the trajectories of type (a) and (b), we have to account for the long trajectories associated with "short" chords of the type (c) but whose centers are close to $\mathcal{C}$. Hence, as already discussed, for evaluating points close to the energy shell we must use a suitable W for Eq. (8). This is just Berry's scar expansion formula in terms of periodic orbits [12,34,35]. Hence, for small distances $|\mathbf{q}^+-\mathbf{q}^-|$, we write

$$C_\varepsilon(\mathbf{q}^+,\mathbf{q}^-,E) = \sum_{\substack{j\in\text{``long''}\\\text{chords}}} C_\varepsilon^j(\mathbf{q}^+,\mathbf{q}^-,E) + C_\varepsilon^0(\mathbf{q}^+,\mathbf{q}^-,E)$$

$$+ C_\varepsilon^{\text{scar}}(\mathbf{q}^+,\mathbf{q}^-,E),$$

(43)

where C_ε^j stands for the jth type (a) orbit corresponding to a term in the sum in Eq. (31), C_ε^0 for the type (b) trajectory term given by Eq. (39), and $C_\varepsilon^{\text{scar}}$ is the result of Eq. (8) for W taken as the scar expansion formula. We do not intend to present here any detailed analysis of this integration, but it is easy to realize that the final result will be an expansion in terms of all the periodic orbits that pass through the points $\mathbf{q}^\pm$. Such conjecture is further supported by noting that when $\mathbf{q}^- = \mathbf{q}^+ = \mathbf{q}$ the integration Eq. (8) reduces to the projection "down" $\mathbf{p}$ of the Berry's scar expansion. The latter case corresponds to Bogomolny formula [11] for scars in the probability density in configuration space, which involves all the periodic orbits that pass through the point $\mathbf{q}$ (see Ref. [34]).

In the other limit, when $|\mathbf{q}^+-\mathbf{q}^-|$ is large, the centers $\mathbf{x}_j$ of all the chords sketched in Fig. 3 are far from $\mathcal{C}$, and we thus write

$$C_\varepsilon(\mathbf{q}^+,\mathbf{q}^-,E) = \sum_{j\neq 0} C_\varepsilon^j(\mathbf{q}^+;\mathbf{q}^-,E) + C_\varepsilon^0(\mathbf{q}^+,\mathbf{q}^-,E),$$

(44)

where we separate the contribution C_ε^0 of the shortest trajectory given by the uniform expression (39).

It is interesting to note that both formulas (43) and (44) imply that the spectral autocorrelation function has contributions arising from W taken at points $\mathbf{x}_j$ well inside the energy shell. In the case of Eq. (43) these are the trajectories with tips on "long" chords. In general, these contributions cannot be neglected, as already discussed at the end of Sec. II. Particularly, the "off-shell" scars of the spectral Wigner function [15] provide the only periodic orbit contributions for C_ε in the case of large separation $|\mathbf{q}^+-\mathbf{q}^-|$.

C. Spatial averaging with $\varepsilon < \varepsilon_{\text{large}}$

We now investigate the effect of spatial averaging on the spectral autocorrelation function. We are interested to know under which circumstances this averaging washes out the

system specific features, allowing one to define a local system independent (or universal) regime for C_ε. Furthermore, the additional spatial averaging brings our results into close relation to numerical experiments, such as the ones in Refs. [22,23].

Defining the local spatial average as

$$\langle C_\varepsilon(\mathbf{q}^+,\mathbf{q}^-,E)\rangle_{\mathbf{q}} \equiv \frac{1}{A(\Omega)}\int_\Omega d\mathbf{q}\, C_\varepsilon(\mathbf{q}^+,\mathbf{q}^-,E), \quad (45)$$

where Ω is a configuration space region of surface $A(\Omega)$ (in d dimension), covering many "local" de Broglie wavelengths $\lambda_{\mathbf{q}}$ across. We define $\lambda_{\mathbf{q}} = 2\pi\hbar/p(\mathbf{q})$ in terms of the local momentum $p(\mathbf{q})$, consistent with the semiclassical approximation. The average is restricted to a region Ω of classically small variations of the smooth potential $V(\mathbf{q})$.

The ubiquitous robustness of Berry's expression for the autocorrelation of chaotic wave functions can be attributed to the following. At small separations $|\mathbf{q}^+-\mathbf{q}^-|$ the local space average kills the terms C_ε^j associated with the "long" chords. This suppression is due to the fact that such terms oscillate in a scale smaller (or at most comparable) to the de Broglie wavelength. Indeed, for small separation the "long" chords are almost parallel to the momentum space and thus its centers have $\mathbf{p}_j(\mathbf{q}^+,\mathbf{q}^-,E)\approx 0$ (see Fig. 3). From Eq. (28), $S_j(\mathbf{q}^+,\mathbf{q}^-,E)\approx S_j(\mathbf{x}_j,E)$ and thus the local spatial wavelength in Eq. (31) is approximately

$$\lambda_{j\mathbf{q}}\approx 2\pi\hbar\left|\frac{\partial S_j(\mathbf{x}_j,E)}{\partial\mathbf{q}}\right|^{-1} = \frac{2\pi\hbar}{|\boldsymbol{\xi}_{j\mathbf{p}}|}, \quad j\neq 0. \quad (46)$$

This is just about the de Broglie wavelength since $|\boldsymbol{\xi}_{j\mathbf{p}}| \sim 2p(\mathbf{q})$. Moreover, the requirement of small spatial averaging regions assures that $p(\mathbf{q})$ is approximately constant for $\mathbf{q}$ inside Ω. Consequently, C_ε^0 for small $|\mathbf{q}^+-\mathbf{q}^-|$ coincides with Berry's result and remains unaffected by the local spatial average [40]. Furthermore, if none of the wave functions inside the energy window from which C_ε is built shows a strong visual scar due to periodic orbits, which is often the case, there is no reason to expect a sizeable correction due to $\langle C_\varepsilon^{\rm scar}\rangle_{\mathbf{q}}$. Thus, after the averaging the leading contribution for C_ε would be the local system independent expression Eq. (4).

Extrapolating our semiclassical analysis of $\langle C_\varepsilon(\mathbf{q}^+,\mathbf{q}^-,E)\rangle_{\mathbf{q}}$ to energy smoothings of the order of one energy spacing (i.e., $\varepsilon\sim\varepsilon_{\rm small}$), we find that our results are still consistent with the numerical investigations [22,23] of the autocorrelation function $C(\mathbf{q}^+,\mathbf{q}^-)$ [in this case Eq. (2)] on individual eigenfunctions for small values of $|\mathbf{q}^+-\mathbf{q}^-|$. For instance, in Ref. [23] we observe that the corrections to Eq. (4) given by $\langle C_\varepsilon^{\rm scar}\rangle_{\mathbf{q}}$ are small unless the eigenfunction has a strong visual scar due to a simple periodic orbit. Likewise, as Eq. (4) is symmetric with respect to the orientations of $(\mathbf{q}^+-\mathbf{q}^-)$ for a fixed value of $|\mathbf{q}^+-\mathbf{q}^-|$, the observed angular dependence of $C(\mathbf{q}^+,\mathbf{q}^-)$ [22,23] arrives precisely from $\langle C_\varepsilon^{\rm scar}\rangle_{\mathbf{q}}$.

Before concluding we would like to add that the local spatial average is the mechanism responsible for the elimi-

nation of the contributions of trajectories associated with "long" chords in the Bogomolny scar formula for the spatial probability density [11]. In our formalism, the latter is recovered after making the local average Eq. (45) over the autocorrelation function C_ε, Eq. (43), and then taking $\mathbf{q}^+ \to \mathbf{q}^-$. In other words, the Bogomolny scar formula captures (in configuration space) only the scar contributions of periodic orbits near the energy shell of the spectral Wigner function, since the "off-shell" scar contributions [15] are washed out by the local spatial average.

IV. CONCLUSIONS

We investigated the spatial two-point autocorrelation of energy eigenfunctions $\psi_n(\mathbf{q})$ corresponding to classically chaotic systems in the semiclassical regime. We use the Weyl-Wigner formalism to obtain the spectral average $C_\varepsilon(\mathbf{q}^+,\mathbf{q}^-,E)$ of $\psi_n(\mathbf{q}^+)\psi_n^*(\mathbf{q}^-)$, defined as the average over eigenstates within an energy window ε centered at E. In the considered framework, C_ε is just the Fourier transform in momentum space of the spectral Wigner function $W(\mathbf{x},E;\varepsilon)$.

The advantage of this formalism comes from the observation that W is almost like tailor made for semiclassical approximations. At each phase space point, $\mathbf{x}\equiv(\mathbf{q},\mathbf{p})$, the semiclassical behavior of W is associated with all the classical trajectories on the energy shell E whose end points are joined by a chord centered at $\mathbf{x}$. These classical contributions are exponentially suppressed when the trajectory traversal time is $t\gtrsim\hbar/\varepsilon$.

In distinction to most studies so far, this paper addresses smooth Hamiltonian systems. Actually, except for Eq. (31) that is for a time reversal symmetric system and Eq. (39) which holds for $H(x)$ of the form Eq. (3), all the formulas in this work are valid for general smooth autonomous Hamiltonians [41]. Our results can evidently be straightforwardly employed to calculate C_ε in billiard systems, where the phase space structure is much simpler than the one considered here. For smooth systems, we show that it is still possible to distinguish in C_ε between a local system independent regime and another one that carries the system classical chord structure information. This is obviously also valid for billiards. The interplay between the spectral average window, which controls the upper time scale of the classical contributions, and the spatial separation scale dictates which aspects prevails. As a result we obtain semiclassical expressions that bridge the existing formulas for the autocorrelation function C_ε.

To the best of our knowledge, the studies of C_ε found in the literature are based on Green's function methods, and employ a given arbitrary separation between "zero-length" and "long" trajectories. In billiards, due to their simplicity, the semiclassical "zero-length" Green's function is an excellent approximation to calculate C_ε, even for ε comparable with $\varepsilon_{\rm large}$, provided that the separation is not too large. In smooth systems corrections accounting for the energy surface curvature become rapidly necessary as the spatial separation is increased. Such corrections, albeit, in principle, feasible to obtain with the Green's function method, are easier to estimate with the here employed framework. This is an

important advantage of the formalism we employ. Our study goes beyond that issue showing that the Wigner-Weyl formalism is a quite general framework for semiclassical approximations, clearly revealing the inextricable relation between the classical chord structure and the choatic wave function correlations.

Note added. Recently, another study of the energy average autocorrelation function $C_\varepsilon(\mathbf{q}^+,\mathbf{q}^-,E)$ has been published [42]. The later improves Hortikar and Srednicki result [27] by normalizing C_ε by the semiclassical local level density. The three terms expression that they found arise from the normalization and bears no relation with our Eq. (43) since our C_ε is not normalized. Obviously, Eq. (43) contains all information of the normalized C_ε.

APPENDIX A: DEMONSTRATION OF EQ. (29)

In this appendix we show that both amplitudes in Eq. (29) are identical, thus proving that Ref. [27] addresses one of the limiting cases of C_ε studied in this paper. For the sake of clarity, it is convenient to express both sides of Eq. (29) in terms of the action defined as $R(\mathbf{q}^+,\mathbf{q}^-,t)=S(\mathbf{q}^+,\mathbf{q}^-,E)-Et$. The variation of R with respect to its independent variables, namely, $\mathbf{q}^+$, $\mathbf{q}^-$, and t gives [3]

$$\mathbf{p}^\pm = \pm \partial R/\partial \mathbf{q}^\pm \quad \text{and} \quad -E = \partial r/\partial t. \tag{A1}$$

It is also convenient to introduce a short notation for the second derivatives of R

$$R_{++} \equiv \frac{\partial^2 R}{\partial \mathbf{q}^{+2}} = \frac{\partial \mathbf{p}^+}{\partial \mathbf{q}^+}, \quad R_{+-} \equiv \frac{\partial^2 R}{\partial \mathbf{q}^+ \partial \mathbf{q}^-} = -\frac{\partial \mathbf{p}^-}{\partial \mathbf{q}^+},$$

$$R_{-+} \equiv \frac{\partial^2 R}{\partial \mathbf{q}^- \partial \mathbf{q}^+} = \frac{\partial \mathbf{p}^+}{\partial \mathbf{q}^-}, \quad R_{--} \equiv \frac{\partial^2 R}{\partial \mathbf{q}^{-2}} = -\frac{\partial \mathbf{p}^-}{\partial \mathbf{q}^-}, \tag{A2}$$

which form a set of four d-dimensional matrices.

With the elements at hand, one readily writes $D(\mathbf{q}^+,\mathbf{q}^-,E)$, as defined in Eq. (30) by a $(d+1)\times(d+1)$-dimensional matrix determinant (see, for instance, Ref. [3])

$$D = \left(\frac{\partial^2 R}{\partial t^2}\right)^{-1} \det(-R_{+-}) = -\left(\frac{\partial t}{\partial E}\right) \det(-R_{+-}). \tag{A3}$$

We switch now to the lhs of Eq. (29). The $(2d\times 2d)$-dimensional stability matrix $\mathcal{M}(\mathbf{x})$ is related to the second derivatives of the action R as follows:

$$\mathcal{M}(\mathbf{x}) = \begin{pmatrix} -R_{+-}^{-1}R_{--} & -R_{+-}^{-1} \\ R_{-+}-R_{++}R_{+-}^{-1}R_{--} & -R_{++}R_{+-}^{1} \end{pmatrix}. \tag{A4}$$

The justification for the above equation can be found in the Appendix A of Ref. [12]. It is now straightforward to show that

$$\det[1+\mathcal{M}(\mathbf{x})] = \frac{\det(R_{+-}-R_{++}-R_{--}+R_{-+})}{\det(-R_{+-})}. \tag{A5}$$

It remains only to express $\partial^2 S/\partial \mathbf{p}^2$ as a function of R to conclude the demonstration. The relation between the second derivatives of the center action $S(\mathbf{q},\mathbf{p},E)$ and the stability matrix $\mathcal{M}(\mathbf{x})$ can be obtained by differentiating $\mathbf{q}^+ \equiv \mathbf{q}^+(\mathbf{q}^-,\mathbf{p}^-)$ and $\mathbf{p}^+ \equiv \mathbf{p}^+(\mathbf{q}^-,\mathbf{p}^-)$ with respect to $\mathbf{q}$ and $\mathbf{p}$. By writing $\mathbf{q}^- = \mathbf{q}^-(\mathbf{q},\mathbf{p})$, $\mathbf{p}^- = \mathbf{p}^-(\mathbf{q},\mathbf{p})$, and recalling that $\mathbf{q}^\pm = \mathbf{q} \mp (\partial S/\partial \mathbf{p})/2$ and $\mathbf{p}^\pm = \mathbf{p} \pm (\partial S/\partial \mathbf{q})/2$, we arrive at

$$[1-\mathcal{J}\mathcal{B}(\mathbf{x})] = \mathcal{M}(\mathbf{x})[1+\mathcal{J}\mathcal{B}(\mathbf{x})], \tag{A6}$$

where

$$\mathcal{B}(\mathbf{x}) = \frac{1}{2}\begin{pmatrix} \dfrac{\partial^2 S}{\partial \mathbf{q}^2} & \dfrac{\partial^2 S}{\partial \mathbf{p}\partial \mathbf{q}} \\ \dfrac{\partial^2 S}{\partial \mathbf{q}\partial \mathbf{p}} & \dfrac{\partial^2 S}{\partial \mathbf{p}^2} \end{pmatrix} \quad \text{and} \quad \mathcal{J} = \begin{pmatrix} 0 & 1 \\ -1 & 0 \end{pmatrix}. \tag{A7}$$

Using the obvious identity $\mathcal{J}^{-1} = -\mathcal{J}$ we recast $\mathcal{B}(\mathbf{x})$ as

$$\mathcal{B}(\mathbf{x}) = -\mathcal{J}[1-\mathcal{M}(\mathbf{x})][1+\mathcal{M}(\mathbf{x})]^{-1}. \tag{A8}$$

The above relation with the aid of Eq. (A4) renders

$$\frac{\partial^2 S}{\partial \mathbf{p}^2} = 2^{2d}(R_{+-}-R_{++}-R_{--}+R_{-+})^{-1}. \tag{A9}$$

Finally, by collecting Eqs. (A3), (A5), and (A9) we arrive at

$$-\left(\frac{\partial t}{\partial E}\right)\left\{\det[1+\mathcal{M}(\mathbf{x})]\det\left(\frac{\partial^2 S}{\partial \mathbf{p}^2}\right)\right\}^{-1}$$

$$= -\left(\frac{\partial t}{\partial E}\right)\frac{\det(-R_{+-})}{2^{2d}}$$

$$= \frac{D}{2^{2d}}, \tag{A10}$$

which proves Eq. (29).

APPENDIX B: DERIVATION OF THE UNIFORM APPROXIMATION EQ. (39)

In this appendix we evaluate the integral Eq. (36) by the uniform approximation method to obtain Eq. (39) for the spectral autocorrelation function. As already mentioned, the integral in Eq. (36) is dominated by its stationary phase points $\pm t_0(\theta,E)$ (solutions of $\partial R_0/\partial t + E = 0$), that coalesce

at the origin as $\theta \to 0$. Thus, we start analyzing the structure of the phase $\Phi(t,\theta)$ and the amplitude $g(t)$ near $t=0$.

For $\Phi(t,\theta)$ we replace the action R_0 by the one found in Eq. (35). We then expand the center action $S_0(\mathbf{x},t)$ [providing that $\mathbf{p}_0 \equiv \mathbf{p}_0(\mathbf{q}^+,\mathbf{q}^-,t)$ is fixed by the condition Eq. (34)], up to third order in t, as in Eq. (19). If the system Hamiltonian has the form of Eq. (3), the expansion reads

$$S_0(\mathbf{x},t) \approx -tH(\mathbf{x}) - \frac{1}{24}t^3 \left(\frac{1}{m}\left|\frac{\partial V}{\partial \mathbf{q}}\right|^2 + \frac{1}{m^2}\mathbf{p}\frac{\partial^2 V}{\partial q^2}\mathbf{p}\right),$$ (B1)

so for Eq. (34) we have

$$-\left.\frac{\partial S_0}{\partial \mathbf{p}}\right|_{\mathbf{x}=\mathbf{x}_0} = \frac{t}{m}\mathcal{A}(\mathbf{q},t)\mathbf{p}_0 = (\mathbf{q}^+ - \mathbf{q}^-),$$ (B2)

where $\mathbf{x}_0 = (\mathbf{q},\mathbf{p}_0)$, with $\mathbf{q} = (\mathbf{q}^+ + \mathbf{q}^-)/2$ and $\mathcal{A}$ is the $(d \times d)$-dimensional matrix

$$\mathcal{A}(\mathbf{q},t) = \mathbb{1} + \frac{t^2}{12m}\frac{\partial^2 V}{\partial \mathbf{q}^2}(\mathbf{q}).$$ (B3)

Solving Eq. (B2) for $\mathbf{p}_0$ and using that $\mathcal{A}^{-1} = \mathbb{1} - (t^2/12m)\partial^2 V/\partial \mathbf{q}^2 + O(t^4)$, we arrive at

$$\mathbf{p}_0(\mathbf{q}^+,\mathbf{q}^-,t) = \frac{m}{t}(\mathbf{q}^+ - \mathbf{q}^-) - \frac{t}{12}\frac{\partial^2 V}{\partial \mathbf{q}^2}(\mathbf{q}) + \mathcal{O}(t^3),$$ (B4)

where $m(\mathbf{q}^+ - \mathbf{q}^-)/t$ comes from the first order term in the t expansion of the center action Eq. (B1). Equations (B1) and (B4) yield

$$\Phi(t,\theta) = \frac{m}{2t}|\mathbf{q}^+ - \mathbf{q}^-|^2 + [E - V(\mathbf{q})]t + \tilde{\Phi}(t,\theta).$$ (B5)

Here the explicit part of Φ arises from the lowest order in Eq. (B1) and $\tilde{\Phi}(t,\theta)$ is an analytical function of t. The phase $\Phi(t,\theta)$ has a pole of order one at the origin of the complex plane t.

The behavior of $g(t)$, defined by Eq. (37), near $t=0$ is dominated by

$$\left|\det\left(\frac{\partial^2 S_0(\mathbf{x},t)}{\partial \mathbf{p}^2}\right)\right|^{-1/2}_{\mathbf{x}=\mathbf{x}_0} \approx \frac{m^{d/2}}{|t|^{d/2}}|\det[\mathcal{A}(\mathbf{q},t)]|^{-1/2},$$ (B6)

as seen from Eq. (B2). For clarity purposes we introduce $\tilde{g}(t)$ an analytical function of t, defined as $g(t) \equiv \tilde{g}(t)/|t|^{d/2}$.

The center action S_0 and $\mathbf{p}_0(\mathbf{q}^+,\mathbf{q}^-,t)$ are odd function of t [35], and consequently so is the phase $\Phi(t,\theta)$. Since $q(t)$ is an even function of t, we are allowed to express Eq. (36) by

$$\frac{2\Delta}{(2\pi\hbar)^{d/2+1}}\,\text{Re}\,I(\hbar,\theta) \equiv \frac{2\Delta}{(2\pi\hbar)^{d/2+1}}\,\text{Re}\int_0^\infty dt\,\frac{\tilde{g}(t)}{t^{d/2}}$$

$$\times \exp\left[\frac{i}{\hbar}\Phi(t,\theta) - id\frac{\pi}{4}\right],$$ (B7)

where we used that $\nu_0(t) \equiv \text{sgn}[\partial^2 S_0(\mathbf{x},t)/\partial \mathbf{p}^2]$, which is the difference between the number of the positive and negative eigenvalues of $\partial^2 S_0(\mathbf{x},t)/\partial \mathbf{p}^2$ and is simply equal to $-td/|t|$ when the energy shell is convex (the case considered in this study). We have now to deal with a single stationary phase point $t_0(\theta,E)$, that coalesces with the lowest limit of the integration, and for which the stationary phase reads

$$\Phi(t_0,\theta) = R_0(\mathbf{q}^+,\mathbf{q}^-,t_0) + Et_0 \equiv S_0(\mathbf{q}^+,\mathbf{q}^-,E).$$ (B8)

The uniform approximation [37] to Eq. (B7) involves the suitable change of the integration variable, $w \equiv w(t):[0,+\infty) \to [0,+\infty)$, such that it is invertible and reduces the phase of the integrand to the canonical form

$$\Phi(t,\theta) = \frac{1}{2}\left(w + \frac{z^2(\theta)}{w}\right) \equiv \phi(w,\theta),$$ (B9)

adhering to $\Phi(t,\theta)$ as given by Eq. (B5). Likewise, we must require that the stationary points $\pm t_0$ of Φ correspond to the saddle points $\pm w_0 \equiv \pm z(\theta)$ of ϕ [i.e., $\partial\phi/\partial w|_{w=\pm w_0} = 0$ for $\pm w_0 = w(\pm t_0)$]. This is achieved by making $z(\theta) = S_0(\mathbf{q}^+,\mathbf{q}^-,E)$ [see Eq. (B8)]. Thus, after the change of variable the integral in Eq. (B7) becomes

$$I(\hbar,\theta) = \int_0^\infty dw\,\frac{\tilde{G}(w)}{w^{d/2}}\exp\left[\frac{i}{\hbar}\phi(w,\theta) - id\frac{\pi}{4}\right],$$ (B10)

where

$$\frac{\tilde{G}(w)}{|w|^{d/2}} = \frac{\tilde{g}(t)}{|t|^{d/2}}\left|\frac{\partial t}{\partial w}\right|,$$ (B11)

and $\tilde{G}$ is an even analytical function of w. In general the next step of the method of uniform approximation is to expand $\tilde{G}$ around w_0 [37], but in our case is sufficient to keep only the first term, namely,

$$\tilde{G}(w) \approx \tilde{G}(w_0) = g(t_0 \equiv t(w_0))\left|\frac{\partial t}{\partial w}\right|_{w=w_0}|w_0|^{d/2},$$ (B12)

where

$$\left|\frac{\partial t}{\partial w}\right|_{w=w_0} = \frac{|\partial\phi/\partial w||_{w=w_0}}{|\partial\Phi/\partial t||_{t=t_0}} = \frac{1}{|S_0(\mathbf{q}^+,\mathbf{q}^-,E)|^{1/2}}\left|\frac{\partial t_0}{\partial E}\right|^{1/2}.$$ (B13)

The last equality was obtained by applying the L' Hospital rule. Now, recalling Eq. (29) we write

$$\widetilde{G}(w_0) = e^{-\varepsilon|t_0|/\hbar} [D_0(\mathbf{q}^+, \mathbf{q}^-, E)]^{1/2} S_0(\mathbf{q}^+, \mathbf{q}^-, E)^{(d-1)/2},$$
(B14)

and using an integral representation of the Hankel's function $H_\nu^{(1)}(z)$ [38], we have

$$I(\hbar, \theta) \approx \frac{\pi G(w_0)}{S_0(\mathbf{q}^+, \mathbf{q}^-, E)^{d/2-1}} H_{d/2-1}^{(1)} \left[\frac{S_0(\mathbf{q}^+, \mathbf{q}^-, E)}{\hbar} \right].$$
(B15)

Finally, collecting the results of Eqs. (B15) and (B14) and taking the real part in Eq. (B7) we obtain the uniform approximation to Eq. (39).

APPENDIX C: DEMONSTRATION OF EQS. (40) AND (41)

In this appendix we derive Eqs. (40) and (41), approximate expressions for the action $S_0(\mathbf{q}^+, \mathbf{q}^-, E)$ and the determinant D_0, respectively. Both relations are valid provided the control parameter $\theta \propto |\mathbf{q}^+ - \mathbf{q}^-|$ is small. Equations (40) and (41) show that our result for the spectral autocorrelation function Eq. (39) reduces to the Berry's one.

Let us start with Eq. (40). The action S_0 is given by Eq. (B8) where t_0 is determined by the stationary phase condition $\partial R_0/\partial t = -E$. For θ small, R_0 is

$$R_0(\mathbf{q}^+, \mathbf{q}^-, t) \approx \frac{m}{2t} |\mathbf{q}^+ - \mathbf{q}^-|^2 - V(\mathbf{q})t$$
(C1)

[see Eq. (B5) and the discussion preceding it]. The stationary phase point t_0 is thus

$$t_0 \approx \frac{m}{p_0(\mathbf{q})} |\mathbf{q}^+ - \mathbf{q}^-|,$$
(C2)

where $p_0(\mathbf{q}) = \sqrt{2m[E - V(\mathbf{q})]}$. By using Eq. (C1) and Eq. (C2) in Eq. (B8) we arrive to the approximation Eq. (40).

For the determinant D_0, from Eq. (A10) we write

$$|D_0(\mathbf{q}^+, \mathbf{q}^-, E)|^{1/2} = 2^d \left| \frac{\partial t_0}{\partial E} \right|^{1/2} |\det[1 + \mathcal{M}_0(\mathbf{x}, t_0)]|^{-1/2}$$

$$\times \det \left(\frac{\partial^2 S_0(\mathbf{x}, t_0)}{\partial \mathbf{p}^2} \right)^{-1/2} \Bigg|_{\mathbf{x} = \mathbf{x}_0}$$
(C3)

where $\mathbf{x}_0 = (\mathbf{q}, \mathbf{p}_0)$ is the center of the shortest chord with tips on a classical trajectory (see Sec. III A). We used the center action $S(\mathbf{x}, t)$ instead of $S(\mathbf{x}, E)$ because for any of both $\boldsymbol{\xi}_\mathbf{q}(\mathbf{x}) = -\partial S/\partial \mathbf{p}$. When $\theta \to 0$, the center $\mathbf{x}_0$ approaches the energy shell, the chord $\boldsymbol{\xi}_0 \approx t_0 \dot{\mathbf{x}}$ [t_0 is given by Eq. (C2)] well approximate the classical trajectory in phase space, and hence $\mathcal{M}_0$ becomes the identity map, yielding

$$\left| \frac{\partial t_0}{\partial E} \right|^{1/2} = \left| \frac{\partial^2 R_0}{\partial t^2} \right|^{-1/2} \Bigg|_{t=t_0} \approx \frac{m}{p_0(\mathbf{q})^{3/2}} |\mathbf{q}^+ - \mathbf{q}^-|^{1/2}, \quad \text{(C4)}$$

where we used Eq. (C1) for R_0. Up to the same order considered in Eq. (C1), the matrix $\mathcal{A}$ in Eq. (B6) becomes the identity and

$$\left| \det \left(\frac{\partial^2 S_0(\mathbf{x}, t_0)}{\partial \mathbf{p}^2} \right)^{-1/2} \right|_{\mathbf{x} = \mathbf{x}_0} \approx \frac{m^{d/2}}{|t_0|^{d/2}} = \frac{p_0(\mathbf{q})^{d/2}}{|\mathbf{q}^+ - \mathbf{q}^-|^{d/2}}.$$
(C5)

Collecting these results in Eq. (C3) we arrive at Eq. (41).

[1] See, for instance, *Supersymmetry and Trace Formulae*, edited by I. V. Lerner, J. P. Keating, and D. E. Khmelnitskii (Kluwer, New York, 1997).

[2] O. Bohigas, M. J. Giannoni, and C. Schmit, Phys. Rev. Lett. **52**, 1 (1984).

[3] M. C. Gutzwiller, *Chaos in Classical and Quantum Mechanics* (Springer-Verlag, New York, 1990).

[4] M. V. Berry, Proc. R. Soc. London, Ser. A **400**, 229 (1985).

[5] E. Bogomolny and J. P. Keating, Phys. Rev. Lett. **77**, 1472 (1996).

[6] A. M. Ozorio de Almeida, C. H. Lewenkopf, and E. R. Mucciolo, Phys. Rev. E **58**, 5693 (1998).

[7] M. L. Mehta, *Random Matrices*, 2nd ed. (Academic, New York, 1991).

[8] B. A. Muzykanskii and D. E. Khmelnitskii, JETP Lett. **62**, 76 (1995).

[9] A. V. Andreev, O. Agam, B. D. Simons, and B. L. Altshuler, Phys. Rev. Lett. **76**, 3947 (1996); A. V. Andreev, B. D. Simons, O. Agam, and B. L. Altshuler, Nucl. Phys. B **482**, 536 (1996).

[10] E. J. Heller, Phys. Rev. Lett. **53**, 1515 (1984).

[11] E. B. Bogomolny, Physica D **31**, 169 (1988).

[12] M. V. Berry, Proc. R. Soc. London, Ser. A **423**, 219 (1989).

[13] L. Kaplan and E. J. Heller, Ann. Phys. (Paris) **264**, 171 (1998).

[14] L. Kaplan, Nonlinearity **12**, R1 (1999).

[15] F. Toscano, M. A. M. de Aguiar, and A. M. Ozorio de Almeida, Phys. Rev. Lett. **86**, 59 (2001).

[16] M. V. Berry, J. Phys. A **10**, 2083 (1977).

[17] A. I. Shnirelman, Usp. Mat. Nauk. **29**, 181 (1974).

[18] A. Voros, Ann. Inst. Henri Poincare, Sect. A **24**, 31 (1976).

[19] V. N. Prigodin, K. B. Efetov, and S. Iida, Phys. Rev. Lett. **71**, 1230 (1993); V. N. Prigodin, B. L. Altshuler, K. B. Efetov, and S. Iida, *ibid.* **72**, 546 (1994); V. N. Prigodin, *ibid.* **74**, 1566 (1995).

[20] I. V. Gornyi and A. D Mirlin, e-print cond-mat/0105103.

[21] R. Aurich and F. Steiner, Physica D **64**, 185 (1993).

[22] B. Li and M. Robnik, J. Phys. A **27**, 5509 (1994).

[23] A. Bäcker and R. Schubert, e-print nlin-CD/0106018.

[24] V. N. Prigodin, N. Tanigushi, A. Kudrolli, V. Kidambi, and S. Sridhar, Phys. Rev. Lett. **75**, 2392 (1995).

[25] B. Eckhardt, U. Dörr, U. Kuhl, and H.-J. Stöckmann, Europhys. Lett. **46**, 134 (1999).

[26] M. Srednicki and F. Stiernelof, J. Phys. A **29**, 5817 (1996).

[27] S. Hortikar and M. Srednicki, Phys. Rev. Lett. **80**, 1646 (1998); Phys. Rev. E **57**, 7313 (1998).

[28] Y. Alhassid and C. H. Lewenkopf, Phys. Rev. B **55**, 7749 (1997).

[29] R. O. Vallejos, C. H. Lewenkopf, and E. R. Mucciolo, Phys. Rev. B **60**, 13 682 (1999).

[30] E. Narimanov, N. R. Cerruti, H. U. Baranger, and S. Tomsovic, Phys. Rev. Lett. **83**, 2640 (1999).

[31] L. Kaplan, Phys. Rev. E **62**, 3476 (2000).

[32] E. Narimanov, H. U. Baranger, N. R. Cerruti, and S. Tomsovic, e-print cond-mat/0101034.

[33] E. P. Wigner, Phys. Rev. **40**, 749 (1932).

[34] M. V. Berry, in *Chaos and Quantum Physics*, Proceedings of the Les Houches Summer School Session L.11, edited by M. J. Giannoni, A. Voros, and J. Zinn-Justin (North-Holland, Amsterdam, 1991), p. 251.

[35] A. M. Ozorio de Almeida, Phys. Rep. **295**, 265 (1998).

[36] M. V. Berry, Adv. Phys. **25**, 1 (1976).

[37] N. Bleistein and R. A. Handelsman, *Asymptotic Expansions of Integrals* (Dover, New York, 1986).

[38] M. Abramowitz and I. A. Stegun, *Handbook of Mathematical Functions* (Dover, New York, 1964); I. S. Gradshteyn and I. M. Ryzhik, *Table of Integrals, Series, and Products*, 2nd ed. (Academic, New York, 1994).

[39] M. V. Berry, Proc. R. Soc. London, Ser. A **424**, 279 (1989).

[40] For billiard systems $p(\mathbf{q})$ is effectively constant so the average area Ω can be taken as the whole billiard area.

[41] Corrections due to not-convex regions of the energy shell have to be taken into account.

[42] B. Li and D. C. Rouben, J. Phys. A **34**, 7381 (2001).